

# Pectin coated iron oxide nanocomposite - a vehicle for controlled release of curcumin

Mausumi Ganguly and Deepika Pramanik

**Abstract**--We report a nanocomposite system capable of efficient drug loading and drug release. The water-soluble iron oxide nanoparticles (IONPs) with particle sizes up to 27 nm were obtained via co-precipitation method. These nanoparticles were coated with pectin to avoid their chances of agglomeration and also to increase the biocompatibility. The nanocomposites obtained were characterized using transmission electron microscopy (TEM), Fourier transform infrared spectroscopy (FT-IR), scanning electron microscopy (SEM), X-ray powder diffraction (XRD) and zeta-potential measurements. The nanocomposite was used to load curcumin, an anticancer compound. The drug loading efficiency of the nanocomposite preparation was evaluated. The drug release from the nanocomposite matrix was studied at four different pH values. The results indicated that the release of drug was not significant in acidic pH but occurred at a uniform and desired rate in alkaline pH. Thus the prepared nanocomposite can act as a vehicle for controlled drug delivery.

**Keywords**--Curcumin, Pectin, Nanoparticles, Drug delivery, Iron oxide.

## I. INTRODUCTION

**N**ANOPARTICLES are particles in the nanosize range ( $10^{-9}$  m), usually 10-100 nm in size. Nano-sized materials display properties that differ from their respective bulk counterparts. Magnetic nanoparticles are useful particles with potential application in medical, biomedical and environmental fields [1]. The nature, sizes, purity and composition of the nanoparticles play important role in their biomedical applications. These particles exhibit unique properties due to their small size and large surface area characteristics, which can be used for drug delivery.

Nanoparticles are capable to reach the sub cellular level as most of the apertures, openings, and gates at cellular or sub cellular levels are of nanometer size [2]. Therapeutic agents are attached to the surface of magnetic nanoparticles or encapsulated within a nanocomposite mixture of a polymer and magnetic nanoparticles. The particles loaded with the drug may be concentrated at the target site and can be operated under the influence of very low values of applied magnetic field. The drugs are then released on the desired area. This approach results in concomitant reduction in quantity of the drug administered and dosage toxicity, enabling the safe

delivery of toxic therapeutic drugs and protection of non target tissues and cells from severe side effects. Treatment with nano particle system increases bio-availability, reduces administration frequency and promotes drug targeting.

Maghemite ( $\gamma$ - $\text{Fe}_2\text{O}_3$ ) and magnetite ( $\text{Fe}_3\text{O}_4$ ) are the two most widely used iron oxide nanoparticles with diverse applications. Bare magnetite nanoparticles on account of their large surface area /volume ratio tend to agglomerate. To prevent agglomeration, a variety of polymeric coatings have been applied to nanoparticles. Among the polymeric capping agents, biopolymers are of special interest due to their biocompatibility and biodegradability. Coating is essential because it reduces aggregation of nanoparticles thereby improving their dispersibility, colloidal stability and protects their surface [3]. A coating of pectin on the nanoparticles reduces the interactions of the electrostatic particles and as a result significantly augments the stability of the diffusion colloid [4].

Co-precipitation and thermal decomposition methods have been the two most widely used methods for the synthesis of iron oxide nanoparticles. The thermal decomposition method finds very little application in biological, environmental and biomedical fields because of the use of toxic organic solvents during synthesis. The co-precipitation method is simple, cost-effective, and the nanoparticles obtained are hydrophilic. This method is favoured for biological application due to the use of low temperature, environmental friendly reagents and conditions. The particle sizes in this case are controlled by applying polymer coating.

The most important and simple parameter for characterization of iron oxide nanoparticles is determination of particle diameter and size distributions. Narrow particle size distributions and the absence of particle aggregation are desirable, since the behavior of aggregated particles deviates significantly from that of isolated primary particles [5]-[6].

Curcumin (Fig. 1A) is a widely known natural bioactive polyphenolic compound which is the major component of turmeric. It exhibits both anticancer and cancer prevention activities by suppressing key elements of initiation, promotion, and metastasis of a wide range of cancer. Curcumin nano formulations have shown an enhanced delivery of the drug in biologically active form to various cancer cells [7]. As a drug carrier, MNPs can effectively increase the stability of drugs, protect them from degradation, promote targeting efficacy, and reduce side effects. Curcumin possess poor water solubility as a result it exhibits solubility limited bioavailability which makes it a class II drug [8]. In the present work, curcumin loaded pectin- iron oxide

---

Mausumi Ganguly is with the Department of Chemistry, Cotton University, Guwahati, Assam 781001, India (email: ganguly\_mausumi@rediffmail.com). Deepika Pramanik is with the Department of Chemistry, Cotton University, Guwahati, Assam 781001, India (email: pramanik.deepika@gmail.com).

nanocomposite preparation was tested to evaluate its efficiency as an oral drug delivery vehicle capable of delivering the drug at some particular pH ranges. The bioavailability of curcumin and its release behaviour at different pH ranges was compared to predict the regions of the gastrointestinal tract where the drug may particularly be delivered.

## II. MATERIALS AND METHODS

### A. Materials

Ferric chloride ( $\text{FeCl}_3 \cdot 6\text{H}_2\text{O}$ ) was obtained from Rankem, Avantor Performance Materials India limited, ferrous sulphate ( $\text{FeSO}_4 \cdot 7\text{H}_2\text{O}$ ) was obtained from Merck limited. Commercial pectin was obtained from LOBA Chemie Laboratory reagents and fine Chemicals, Mumbai. All other chemicals were of reagent grade and were used as obtained. Distilled water was used throughout the process and an inert atmosphere was created by the flow of nitrogen gas.

### B. Preparation of pectin coated iron oxide nanoparticles

Magnetic nano composites composed of magnetite nanoparticles in a pectin matrix were synthesized by an *in situ* co-precipitation method [9]-[10]. Powdered pectin was dissolved in double distilled water to obtain pectin solution of different concentration (0.3%, 0.5% and 0.8%) (w/v). An inert atmosphere was initiated by the flow of nitrogen gas. A solution of ferric and ferrous ions in 2:1 molar ratio was prepared by mixing 0.2M  $\text{FeCl}_3 \cdot 6\text{H}_2\text{O}$  and 0.1M  $\text{FeSO}_4 \cdot 7\text{H}_2\text{O}$ . The said solution was added drop wise to the pectin solution under continuous stirring for 2 hours which resulted in a deep brown solution. The reaction mixture was further deoxygenated by the flow of nitrogen gas. Ammonium hydroxide was used as a precipitating agent. The base was added drop wise to the solution until pH becomes 11 and solution turned deep black indicating the formation of magnetite. The solution obtained was irradiated with ultrasound waves for 30 minutes. The nanocomposites obtained were filtered and washed several times with double distilled water until pH dropped to 7. The black precipitate was then dried at room temperature, characterised and stored in a desiccator.



### C. Loading of curcumin in iron oxide-pectin nanocomposite

Curcumin solution was made by dissolving 10mg of the drug in 100mL of 90% ethanol solution. 500mg of the above mentioned powdered nanocomposite was suspended in water and added to the above solution and stirred for 4 hours. The nano composite loaded with drug was dried at room temperature, kept away from moisture, heat and light and stored for further use.

### D. Characterisation

#### (a) FT-IR spectroscopy

FTIR is an appropriate technique to establish the attachment of the polymer to the magnetic nanoparticles and conjugation with the drug. Each sample was ground and mixed with dry potassium bromide (KBr). The spectra was recorded in absorbance mode from 4000-400  $\text{cm}^{-1}$  (mid infrared region) at the resolution of 4  $\text{cm}^{-1}$ .

#### (b) Powder XRD

The crystallinity and phase purity of the nanocomposites formed were determined by powder X-ray diffraction (pXRD) on a Bruker D8 Advance Diffractometer using a  $\text{CuK}\alpha$  radiation source ( $\lambda = 0.15406 \text{ nm}$ , 40 kV and 40 mA).

#### (c) Scanning electron microscope

The morphology of the nanocomposites was determined by scanning electron microscopy on Carl Zeiss Sigma VP instrument.

#### (d) Transmission electron microscope

The particle sizes, size distribution, morphology and shape of maghemite particles were determined by JEOL 2100 operating at 200 KV. TEM samples were prepared by dispersing nanoparticles in acetone for 30 min by ultrasonic vibration. The aqueous dispersion was dropped on a carbon coated copper TEM grid with filter paper underneath to absorb the acetone and dried in vacuum. The particle size distributions were determined from the TEM images using the image J software. The diameter of iron oxide NPs was evaluated by measuring at least 100 particles.

#### (e) Dynamic light scattering

The hydrodynamic size, polydispersity index (PDI) and zeta potential of the prepared nanoparticles in suspension were evaluated by Dynamic Light Scattering (DLS) analysis using Malvern Zeta Sizer Nano Series (Malvern Instruments, UK) according to the manufacturer's instructions. Samples were diluted in ultra-pure water, to avoid multiscattering, to the appropriate concentration. The intensity of the He-Ne laser (633 nm) was measured at an angle of 90°.

### E. In vitro drug loading studies

#### (a) Estimation of curcumin content in the composite

One-hundred milligrams of the microencapsulated product was digested in 100 mL of acetonitrile: buffer (1:1) at room temperature. After digestion, it was diluted, filtered to remove debris and the resulting solution was quantified spectrophotometrically (UV-Vis) at a optimum wavelength of 427 nm, which corresponds to the absorption peak of curcumin.

#### (b) Determination of percentage of drug loading (L%)

The percentage of drug loading can be estimated by using the following formula:

$$L = \frac{Q_m}{W_m} \times 100,$$

where

L is the percentage loading of microcapsules,

Q<sub>m</sub> is the quantity of drug in g present in W<sub>m</sub> g of microcapsules and

W<sub>m</sub> is the weight of microcapsules in g.

### (c) Determination of encapsulation efficiency (EE%)

The amount of curcumin encapsulated in the microcapsules was determined by using the following formula:

$$EE = \frac{Q_p}{Q_t} \times 100,$$

where

EE is the percentage of encapsulation of microcapsules,

Q<sub>p</sub> is the quantity of drug encapsulated in microcapsules (g),

Q<sub>t</sub> is the quantity of drug added for encapsulation (g),

Q<sub>p</sub> is the product of drug content per g of microcapsules and yield of microcapsules (g)

### F. In-vitro release study of drug

In vitro drug release studies were carried out in dissolution rate test equipment (IKON instrument, Delhi, India) at 37°C and 50 rpm speed. Each formulation was immersed in the buffer solutions at appropriate pH and dissolution was carried out for first 8 hours. During the dissolution study 10mL aliquot was withdrawn from the dissolution medium at predetermine time. The absorbance was measured spectrophotometrically. The amount of drug release from the tablet was calculated using the respective calibration curve.

## III. RESULTS AND DISCUSSION

### A. FT-IR studies

The formation of the nanocomposite can be established by comparing the IR spectra (Fig. 1) of bare iron oxide with that obtained after putting it in a pectin solution. In case of uncoated iron oxide, the band at 3414 cm<sup>-1</sup> is assigned to stretching vibrations and the band at 1630cm<sup>-1</sup> is assigned to bending vibrations of the water molecules adsorbed on the surface of the iron oxide nanoparticles. The band observed at 600 cm<sup>-1</sup> corresponds to the stretching vibrations of M<sub>Th</sub>-O-M<sub>Oh</sub>, where M<sub>Th</sub> and M<sub>Oh</sub> correspond to the iron occupying tetrahedral and octahedral positions, respectively. The new peaks at 1586 - 1587 cm<sup>-1</sup> and 1392 - 1394 cm<sup>-1</sup> obtained in the nanocomposite can be attributed to the symmetric and asymmetric stretching of carboxylate-metal (COO-Fe) linkage. COO<sup>-</sup> stretching bands at 1416 cm<sup>-1</sup>, -CH<sub>2</sub>- bending band at 1500 cm<sup>-1</sup>, the intense peak at 1100 cm<sup>-1</sup> arises from the glycosidic bonds linking two galacturonic sugar units and

600 cm<sup>-1</sup> is for iron oxide nanoparticles confirm the attachment of pectin to iron oxide nanoparticles.

FTIR was further extended to study the conjugation of Curcumin with the pectin coated iron oxide nano particles (Fig. 2). The characteristic peaks at 1581 cm<sup>-1</sup>, 1511 cm<sup>-1</sup>, 1279 cm<sup>-1</sup>, and 1152 cm<sup>-1</sup> appearing in the curcumin loaded nanocomposites arise due to the stretching vibrations of the benzene ring, C=C vibrations, aromatic C-O stretching, and C-O-C stretching modes, respectively in curcumin.

### B. XRD studies

The crystalline structure of iron oxide sample was analyzed by observing the XRD pattern (Fig. 3). Phase identification was performed by matching peak positions and relative intensities to reference JCPDS (Joint Committee on Powder Diffraction Standards) files.

The XRD patterns of prepared Fe<sub>3</sub>O<sub>4</sub> show that the diffraction pattern is close to the standard pattern for crystalline magnetite [3]. The characteristic diffraction peaks at 2 θ = 30.54, 36.00, 43.54, 53.82, 57.66 and 63.28 could be indexed by their indices (2 2 0), (311), (4 0 0), (4 2 2), (511), and (4 4 0) respectively which could arise from the inverse cubic spinel structure of Fe<sub>3</sub>O<sub>4</sub> according to JCPDS card no. 85-1436. The crystalline structure of Fe<sub>3</sub>O<sub>4</sub> did not change on modification of the particles with pectin and the pectin coating occurred only at the surface of Fe<sub>3</sub>O<sub>4</sub> MNs and resulted in no detectable chemical or physical change in bulk of the nanoparticles. The particle sizes were quantitatively evaluated from the XRD data using the Debye-Scherrer equation [11],

$$D = \frac{k\lambda}{\beta \cos\theta}$$

where *k* is Scherrer constant (0.89), *λ* the X-ray wavelength (0.15405 nm), *β* the peak width of half-maximum, and *θ* is the Bragg diffraction angle. The average particle size for iron oxide nanoparticle was found to be 33.18 nm and that of pectin coated iron oxide nanoparticle was found to be 15.23 nm.

### C. Scanning electron microscopy (SEM)

SEM was used in order to examine the particle surface morphology and shape. The SEM micrographs of pure Fe<sub>3</sub>O<sub>4</sub> nanoparticles and pectin coated Fe<sub>3</sub>O<sub>4</sub> nanoparticles are shown in Fig. 4. These images showed that the prepared nanoparticles had regular spherical shape and a core-shell structure. Due to large specific surface area and high surface energy, some bare magnetite nanoparticles were aggregated. However, after being coated with pectin, the nanoparticles were well dispersed.

### D. TEM analysis

The TEM images for pure magnetite display the largest particle size distribution with evidence of aggregation of magnetite particles. It could be seen that aggregation is an issue as particles seem to overlap each other in the TEM image creating the dense black portions of the image [12]. Spherical magnetite and maghemite particles offer a uniform surface area for coating and conjugation of targeting ligands or

therapeutic agents. Particles with size range of 10-100nm is considered to be optimum for nano composite drug delivery system. Particles with size smaller than 10nm are removed by renal clearance, while the one greater than 100nm remains concentrated in the spleen or are taken up by phagocytic cells of the body causing decreased plasma concentration in both the case. Therefore control of particle sizes during preparation is an important factor [13]. The diameter of iron oxide NPs was evaluated by measuring at least 100 particles. The particle size distribution for both uncoated and coated iron oxide nanoparticles are shown in Fig. 6.

The average particle size for uncoated iron oxide nanoparticle was found to be **27.13 nm** and that of coated was found to be **16.30 nm**. The chemical composition of iron oxide nanoparticle was investigated by EDX (Energy dispersive X-ray spectroscopy) in TEM. The graph shows two very high peaks which represent carbon and copper (Fig. 7). These two elements are present because they are the basic constituents of the grid: the support and coating. The other peaks represent the iron and oxygen which are the constituents of the iron oxide, components of nanoparticles.

#### E. DLS measurement

The DLS measurement shows the distribution of size of particles with respect to the intensity. It is seen that particle size obtained in this method is many times larger than the size determined from the TEM measurement. TEM micrographs gives the 'true radius' of the particles (though determined on a statistically small sample), and DLS provides the hydrodynamic radius on an ensemble average [14]-[15].

#### F. Zeta potential measurement

$\zeta$  potential is the potential difference between the dispersion medium and stationary layer of fluid attached to the dispersed particle. It measures the surface charge of the colloidal particles and is an important parameter to know the stability of such particles. In general most of the colloidal particles have either positive or negative charges on their surface. As the particle charge density increases, the particle tend to acquire more intensive repulsive force that prevent contact between them [16]. The Table 1 relates the stability of colloids with the  $\zeta$  potential values.

$\zeta$  potential value for uncoated iron oxide nanoparticles was found to be  $-4.55\text{mV}$  while that of pectin coated nanocomposite was found to be  $-35.9\text{mV}$  (Figs. 8a and 8b). These values indicate that pectin coated iron oxide nanoparticles are more stable than the bare iron oxide nanoparticles. Particle aggregation is less likely to occur for charged particles having high zeta potential due to electrostatic repulsion between the charged particles indicating a long term stability. Thus modification of iron oxide nanoparticles with the pectin has altered the charge on the surface of the particles. The charge of MNPs was described as very fundamental parameter because a negative charged surface makes MNPs more biocompatible, while a positive charge increases the interaction between MNPs and cells but is more toxic too.

The polydispersity index (PDI) is an important parameter that measures the variation of size distribution of particles in a sample. PDI value ranges from 0.000 to 0.500. A low PDI value is desirable as the size range becomes wide when the value increases or nearly approaches 0.5. A PDI value greater than 0.5 indicates the aggregation of the nanoparticles [17]. The PDI value for the uncoated nanoparticle was found to be 0.241 and that of the composite was found to be 0.282 ( Figs. 9a and 9b).

Therefore, pectin coating reduced the aggregation and enhanced the particle dispersion. It is an important factor in drug delivery applications that nanoparticles are individually dispersed and are not agglomerated because aggregation would reduce the effective magnetization of nanoparticles and cause difficulties during drug delivery to the desired site.

#### G. Drug loading and in vitro release analysis

Drug can be loaded in pectin nanoparticles by active or passive loading techniques. In active loading drug is loaded during the preparation of particles. In passive loading drug is loaded after the formation of particles. Drug loading is achieved by encapsulating drug on the nanocomposite. Low entrapment efficiency of drug is a major drawback of delivering the drug by coating on the surface on nanocomposite as only a limited amount of drug can be conjugated in this way [18]. Different combinations of iron oxide and pectin ratio were prepared and the one with best loading and encapsulation efficiency (sample no N 0.5) was selected for *in vitro* drug release studies (Table 2 ). The *in vitro* drug release studies of the curcumin loaded pectin coated iron oxide nanocomposite were carried out in different buffer media with pH 2, 4, 7 and 9 ranging from gastric to intestinal pH. The concentration of drug released was determined from the absorbance at **480 nm** (measured using a UV-Vis spectrophotometer) and previously established calibration curves. The drug release pattern is shown in the Fig. 10. The release is plotted as concentration versus time in hours. The figure indicates that in acidic pH ranges the drug release rate is poor and less than 30% of the drug is released in 24 hours time. In neutral pH, the drug release is better and at alkaline pH range i.e, in the simulated intestinal fluid the drug is released in a desired rate. The drug release is up to 80% in the first 48 hours at pH 9. Thus the drug is not delivered in the regions of the digestive tract where the pH is acidic. Moreover, as the drug release is slow, it is not released appreciably in the first few hours and thus the drug is preferentially released in the large intestine and colon where the preparation reaches late. This indicates that the vehicle is suitable for intestine specific or colon specific drug delivery [19].

## IV. CONCLUSIONS

In the present study, an organo-inorganic hybrid system involving iron oxide nanoparticles has been developed for selective delivery of curcumin to the targeted organs. Iron oxide is easily degradable and therefore useful for *in vivo* applications. Attaching curcumin to the nanoparticle based

drug delivery system can increase the bioavailability of the drug.

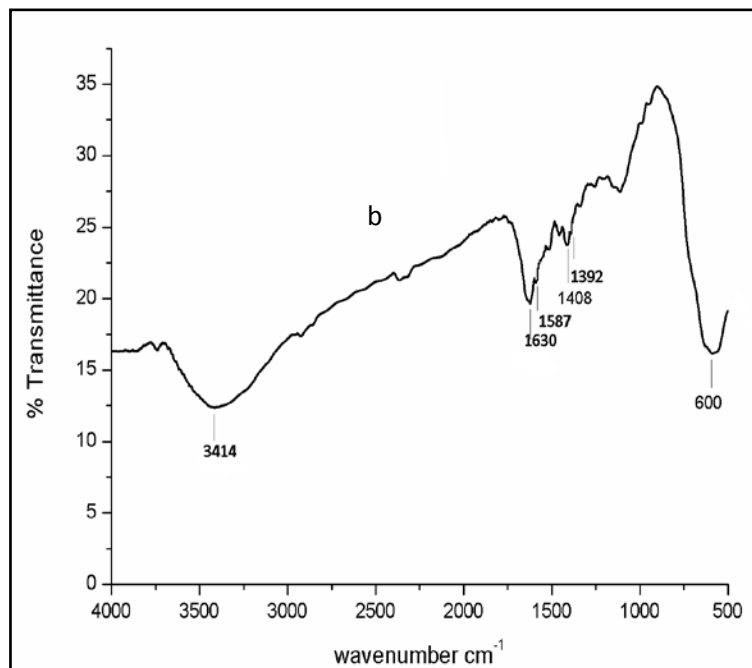
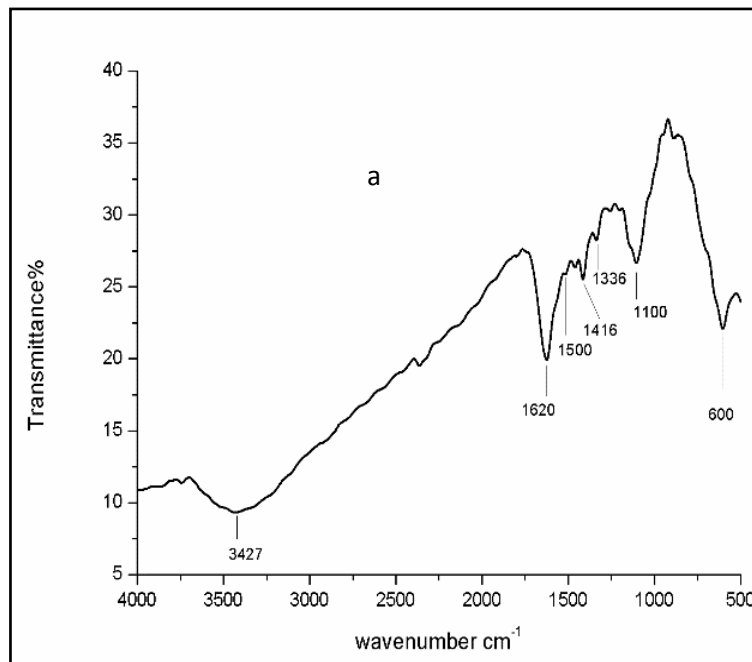
The release profiles of curcumin from the superabsorbent polymer in simulated gastric fluid (pH<2) and in simulated intestinal fluid (pH >7) are different. The drug release was less in acidic medium while it showed sustained release in alkaline medium (pH >7).

Biodegradable pectin-iron oxide preparation could successfully deliver curcumin to the large intestine without losing the drug in the stomach, and could be potential candidate as an orally administrated drug delivery system for colon specific drug delivery.

#### REFERENCES

- [1] F. T. J. Ngenefeme, N. J. Eko, Y. D. Mbom, N. D. Tantoh and K. W. M. Rui, "A one pot green synthesis and characterisation of iron oxide-pectin hybrid nanocomposite," *Open J. Compos. Mater.*, vol. 3, pp. 30-37, 2013.
- [2] M. Sivasankar and B. Kumar, "Role of nanoparticles in drug delivery system," *Int. J. Res. Pharm. Biomed. Sci.*, vol. 1, pp. 41-66, 2010.
- [3] A. Jegan, A. Ramasubbu, S. Saravanan and S. Vasanthkumar, "One-pot synthesis and characterization of biopolymer-iron oxide nanocomposite," *Int. J. Nano Dimens.*, vol. 2, pp. 105-110, 2011.
- [4] Wahajuddin and S. Arora, "Superparamagnetic iron oxide nanoparticles: magnetic nanoplatforms as drug carriers," *Int. J. Nanomedicine.*, vol. 7, pp. 3445-3471, 2012.
- [5] R. Omidirad, F. H. Rajabi and B. V. Farahani, "Preparation and *in vitro* drug delivery response of doxorubicin loaded poly(acrylic acid)-coated magnetite nanoparticles," *J. Serb. Chem. Soc.*, vol. 78, pp. 1609-1616, 2013.
- [6] S. Kayal and R. V. Ramanujan, "Doxorubicin loaded PVA coated iron oxide nanoparticles for targeted drug delivery," *Mater. Sci. Eng. C.*, vol. 30, pp. 484-490, 2010.
- [7] M. M. Yallapu, M. Ebeling, S. Khan, V. Sundram, N. Chauhan, B. K. Gupta, S. E. Puumala, M. Jaggi and S. C. Chauhan, "Novel Curcumin-Loaded Magnetic Nanoparticles for Pancreatic Cancer Treatment," *Mol. Cancer Ther.*, vol. 12, pp. 1471-1480, 2013.
- [8] S. S. Bansal, M. Goel, F. Aqil, M. V. Vadhanam and R. C. Gupta, "Advanced Drug Delivery Systems of Curcumin for Cancer Chemoprevention," *Cancer Prev. Res.*, vol. 4, pp. 1158-1171, 2011.
- [9] J. Namanga, J. Foba, D. T. Ndinteh, D. M. Yufanyi and R. W. M. Krause, "Synthesis and Magnetic Properties of a Superparamagnetic Nanocomposite Pectin-Magnetite Nanocomposite," *J. Nanomater.*, Article ID 137275, 2013.
- [10] M. Farahmandjou and F. Soflaee, "Synthesis of Iron Oxide Nanoparticles using Borohydride Reduction," *Int. J. Bio-Inorg. Hybrid Nanomater.*, vol. 3, pp. 203-206, 2014.
- [11] S. Asgari, Z. Fakhari and S. Berijani, "Synthesis and Characterization of Fe<sub>3</sub>O<sub>4</sub> Magnetic Nanoparticles Coated with Carboxymethyl Chitosan Grafted Sodium Methacrylate," *J. Nanostruct.*, vol. 4, pp. 55-63, 2014.
- [12] N. Sangeetha and A. K. Kumaraguru, "Antitumor effects and characterisation of biosynthesized iron oxide nanoparticles using seaweeds of Gulf of Mannar," *Int. J. Pharm. Pharm. Sci.*, vol. 7, pp. 469-476, 2015.
- [13] A. P. Ranjan, A. Mukherjee, L. Helson and J. K. Vishwanatha, "Scale up, optimization and stability analysis of Curcumin C3 complex-loaded nanoparticles for cancer therapy," *J. Nanobiotechnology.*, vol. 10:38, pp. 1-18, 2012.
- [14] S. S. Behera, J. K. Patra, K. Pramanik, N. Panda and H. Thatoi, "Characterization and Evaluation of Antibacterial Activities of Chemically Synthesized Iron Oxide Nanoparticles," *World J. Nanosci. Eng.*, vol. 2, pp. 196-200, 2012.
- [15] J. Sommertune, A. Sugunan, A. Ahniyaz, R. S. Bejhed, A. Sarwe, C. Johansson, C. Balceris, F. Ludwig, O. Posth and A. Fornara, "Polymer/Iron Oxide Nanoparticle Composites—A Straight Forward and Scalable Synthesis Approach," *Int. J. Mol. Sci.*, vol. 16, pp. 19752-19768, 2015.
- [16] S. C. Yang, S. Y. Paik, J. Ryu, K. O. Choi, T. S. Kang, J. K. Lee, C. W. Song and S. Ko, "Dynamic light scattering-based method to determine primary particle size of iron oxide nanoparticles in simulated gastrointestinal fluid," *Food Chem.*, vol. 161, pp. 185-191, 2014.
- [17] A. P. Gadad, P. Sharath Chandra, P. M. Dandagi and V. S. Mastiholimath, "Moxifloxacin loaded polymeric nanoparticles for sustained ocular drug delivery," *Int. J. Pharm. Sci. Nanotech.*, vol. 5, pp. 1727-1734, 2012.
- [18] C. H. Vineela and S. K. Krishna, "Preparation of Ibuprofen-loaded Eudragit S100 nanoparticles by Solvent evaporation technique," *Int. J. Pharm. Sci. Res.*, vol. 5, pp. 375-384, 2014.
- [19] N. Kumar, A. K. Patel, N. Kumari and A. Kumar, "A review on chitosan nanoparticles for cancer treatment," *Int. J. Nanomater. Biostruct.*, vol. 4, pp. 63-65, 2014.

Fig.1 FTIR spectra of (a) uncoated iron oxide nanoparticles and (b) pectin coated iron oxide nanoparticles



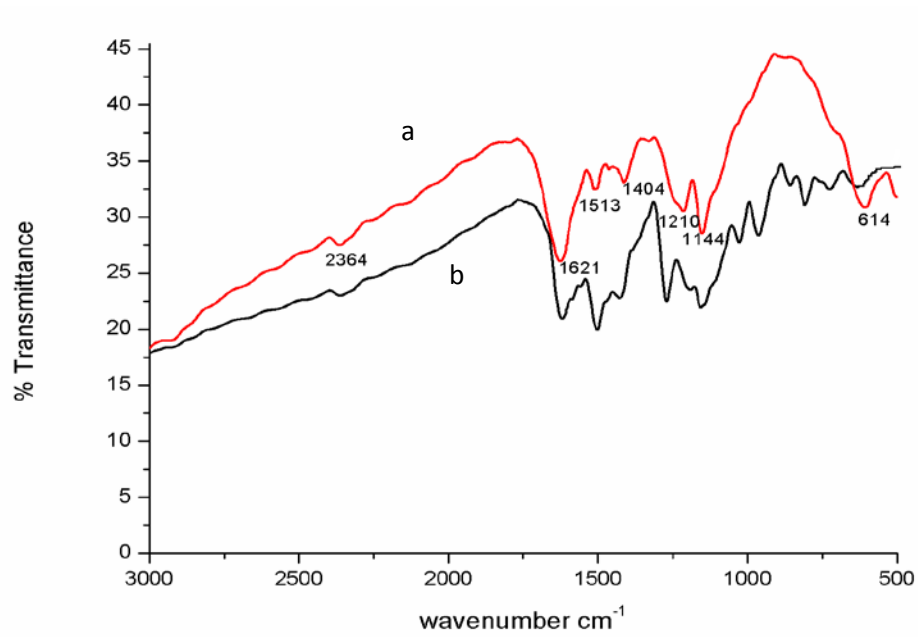
**Fig 2** FTIR spectra of (a) curcumin and (b) curcumin conjugated pectin coated iron oxide nanoparticles.

Fig 3: XRD of (a) iron oxide nanoparticle and (b) pectin coated iron oxide nanoparticle.

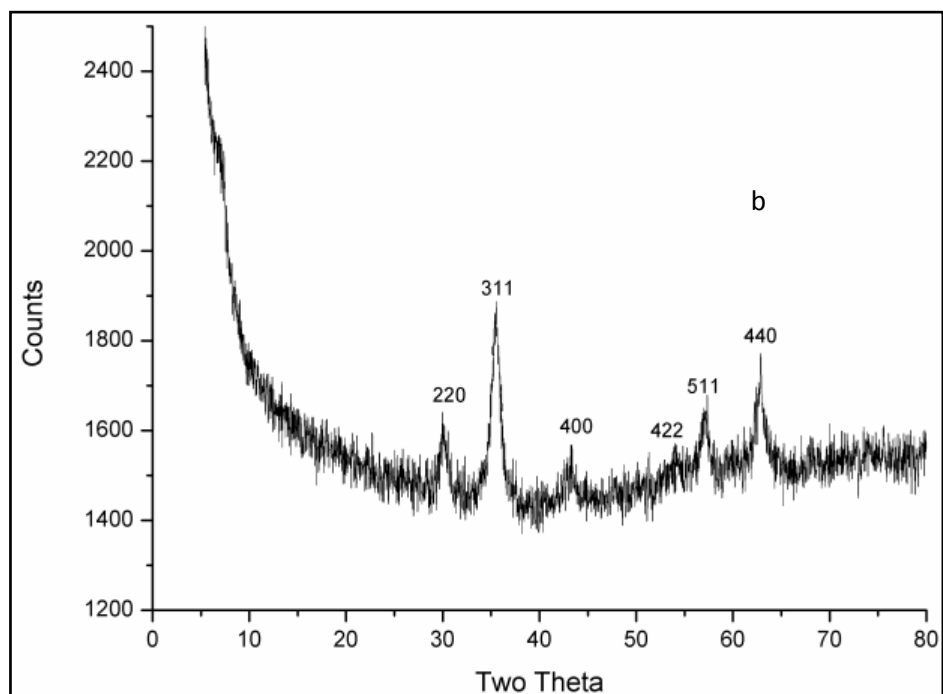
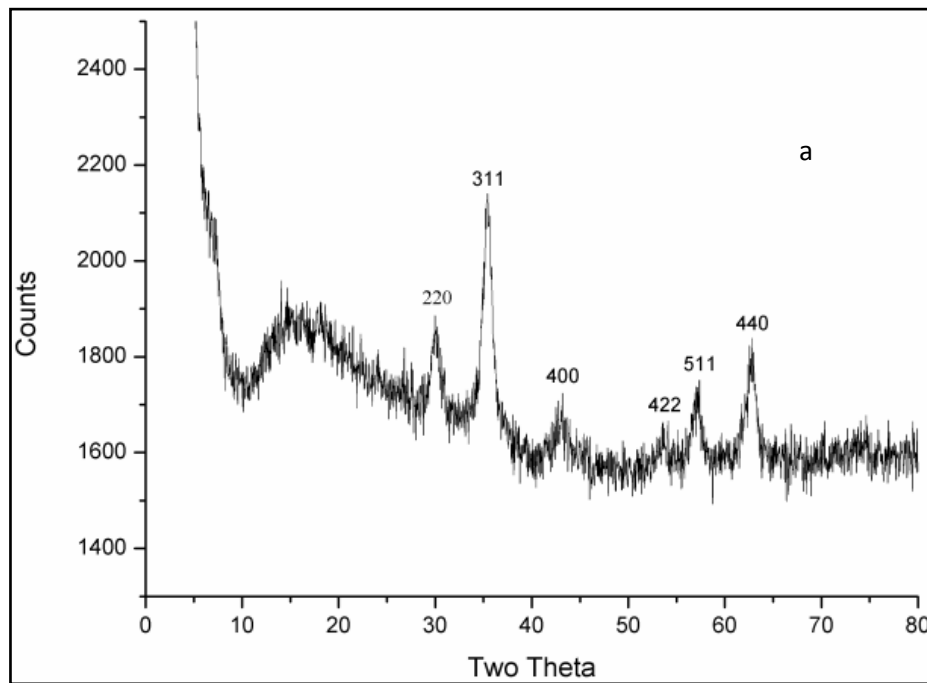


Fig.4 SEM micrographs of pure  $Fe_3O_4$  nanoparticles and pectin coated  $Fe_3O_4$  nanoparticles.

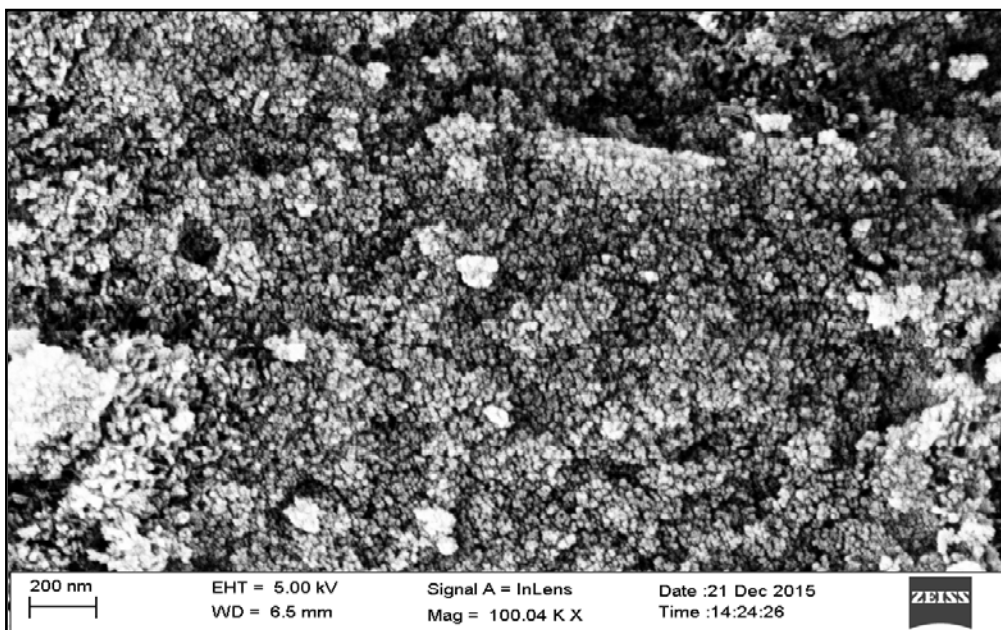
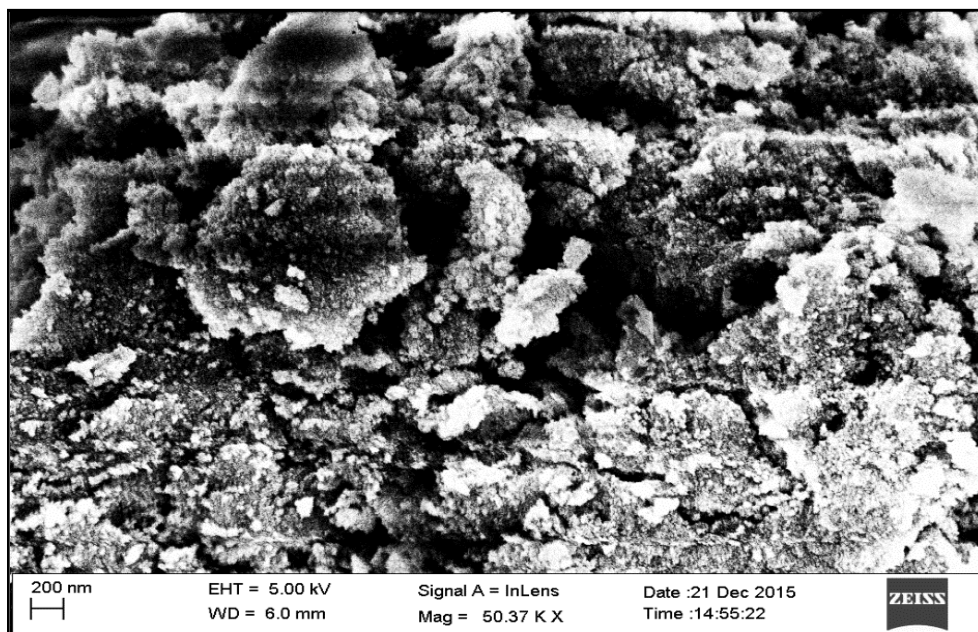


Fig.5 TEM images of uncoated and coated iron oxide nanoparticles.

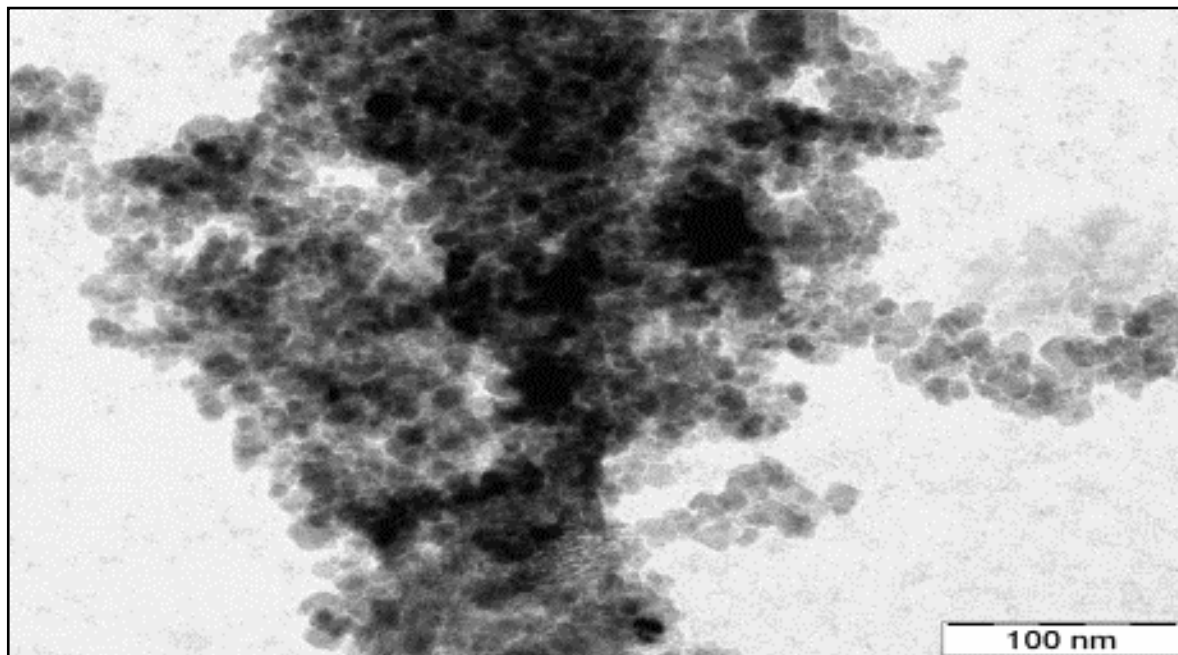
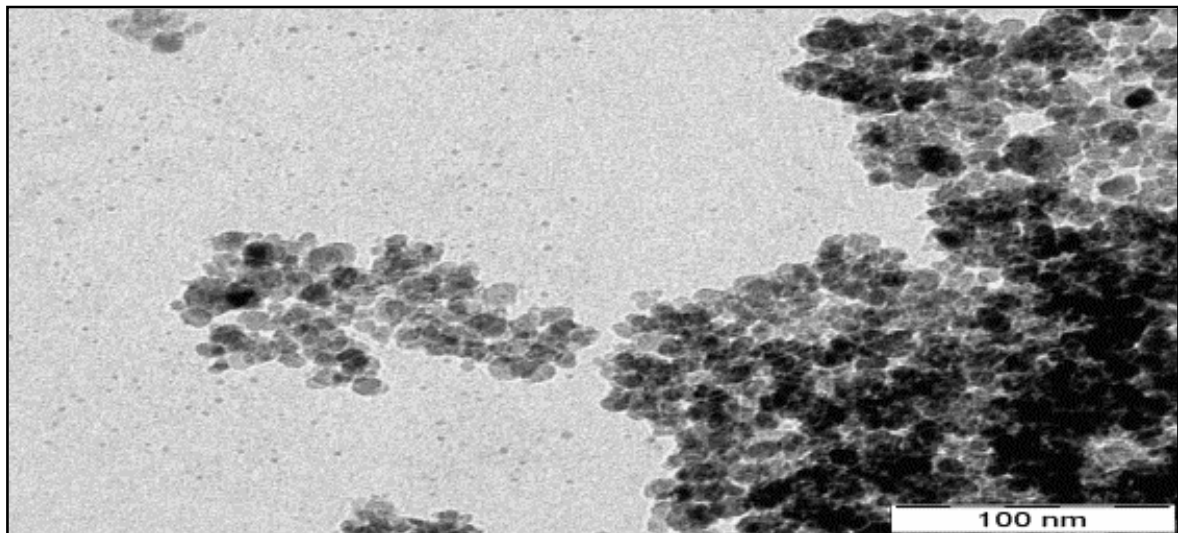


Fig.6 The particle size distribution for both uncoated and coated iron oxide nanoparticles.

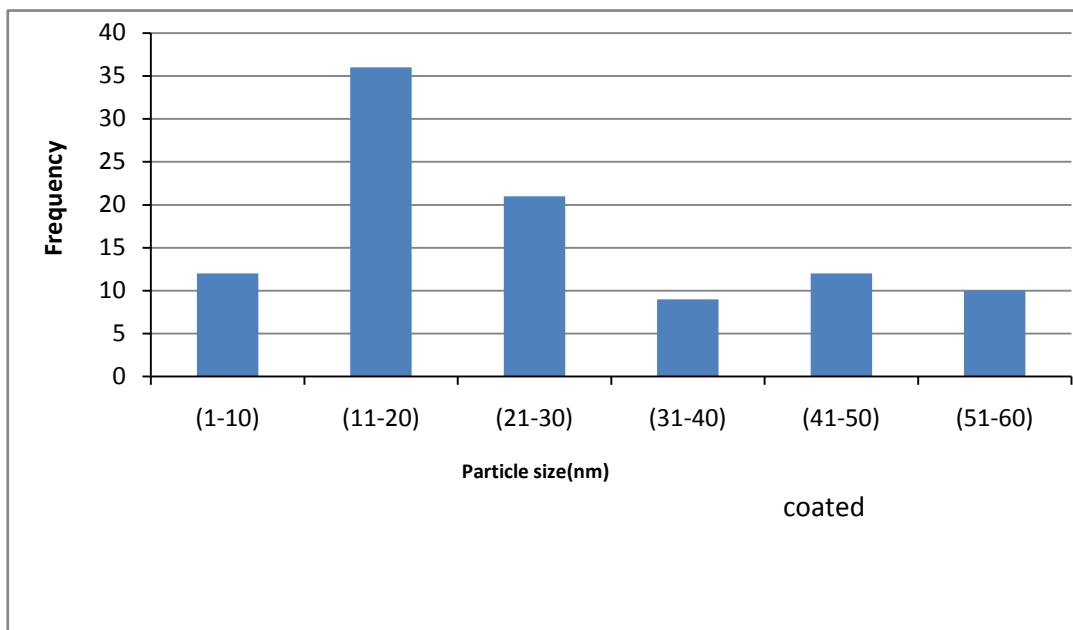
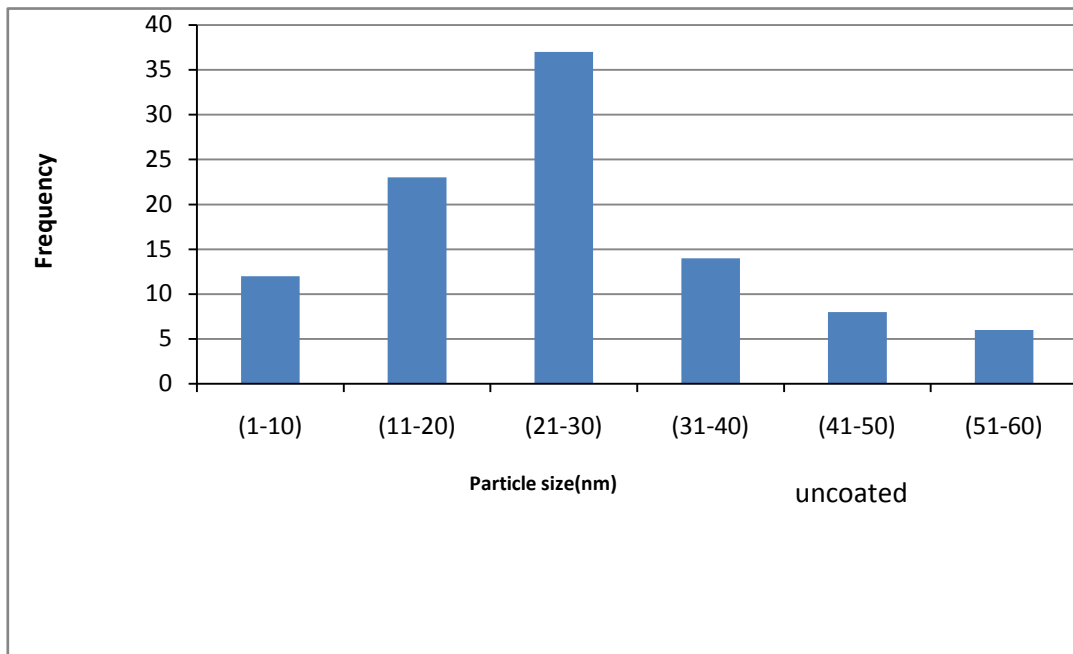


Fig.7 EDX spectra of the nanoparticles.

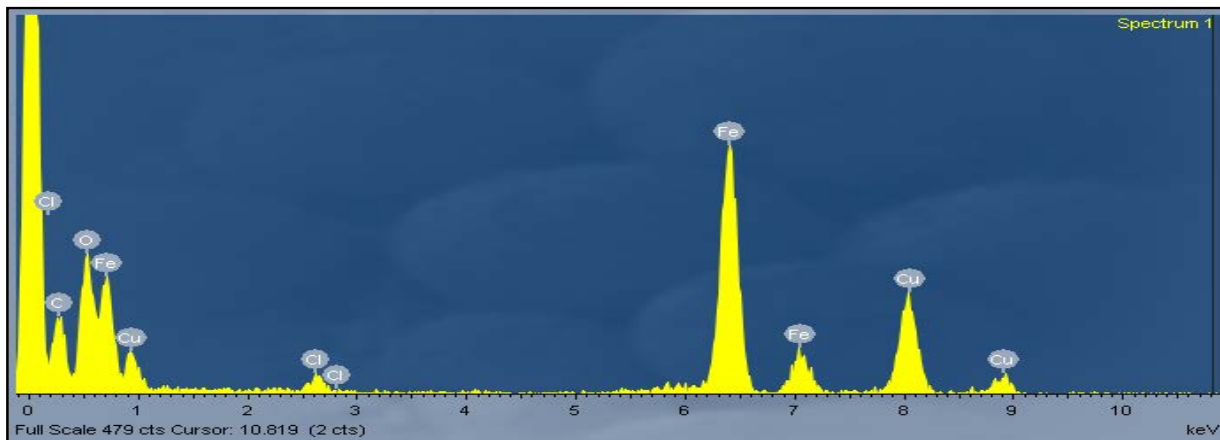


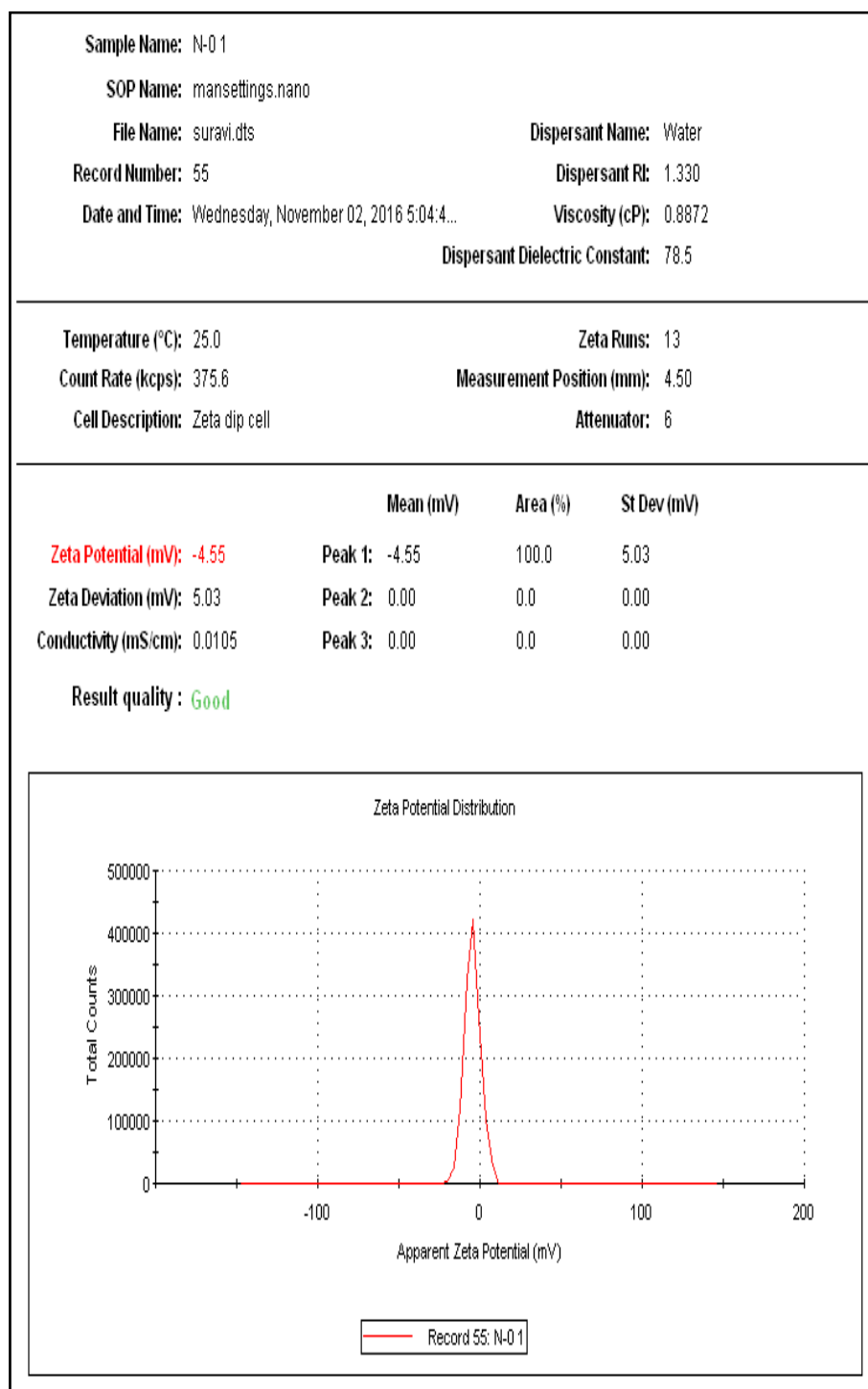
Fig.8a  $\zeta$  potential value for uncoated iron oxide nanoparticles.

Fig.8b  $\zeta$  potential value for coated iron oxide nanoparticles.

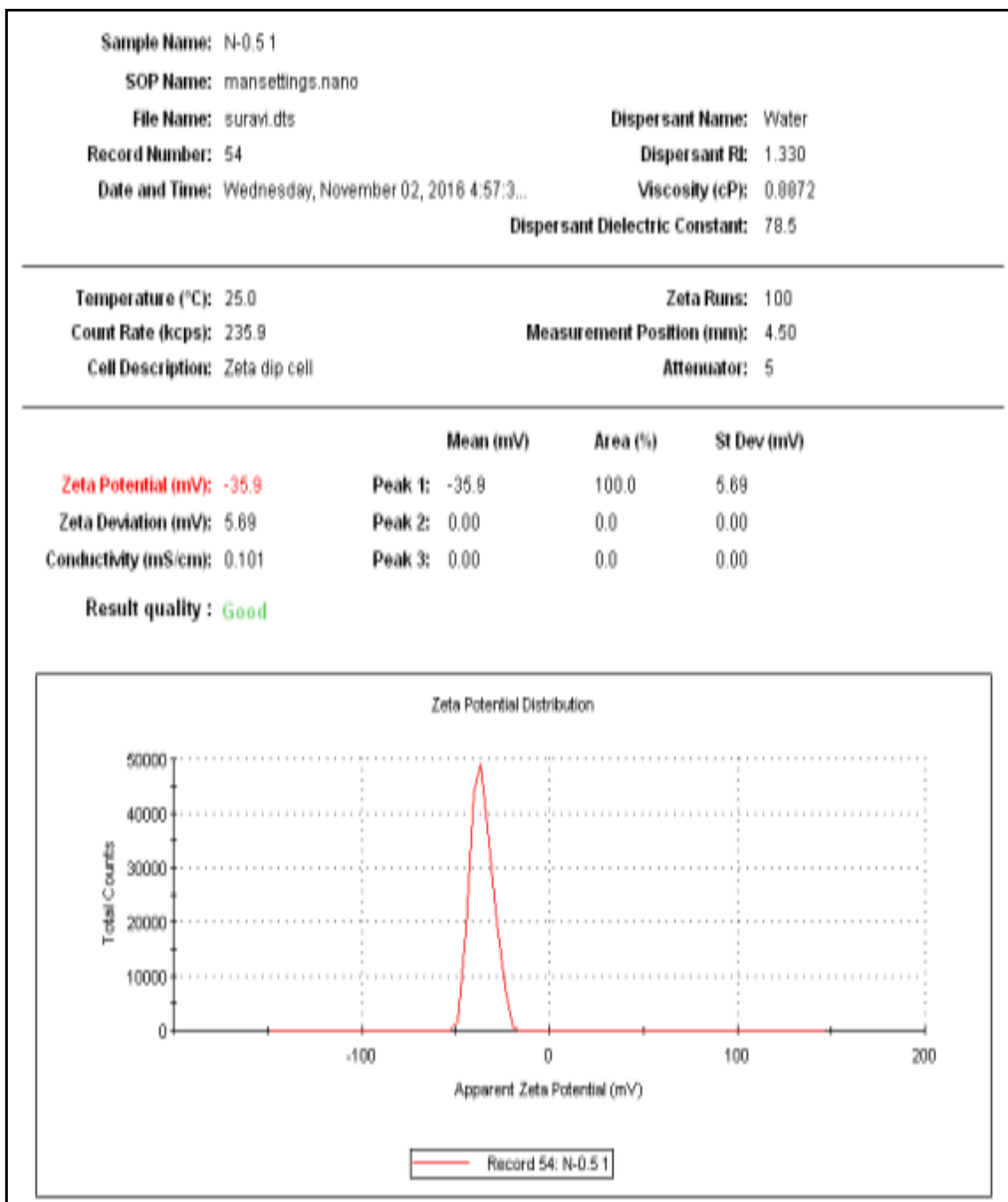


Fig.9a PDI value for the uncoated nanoparticle.

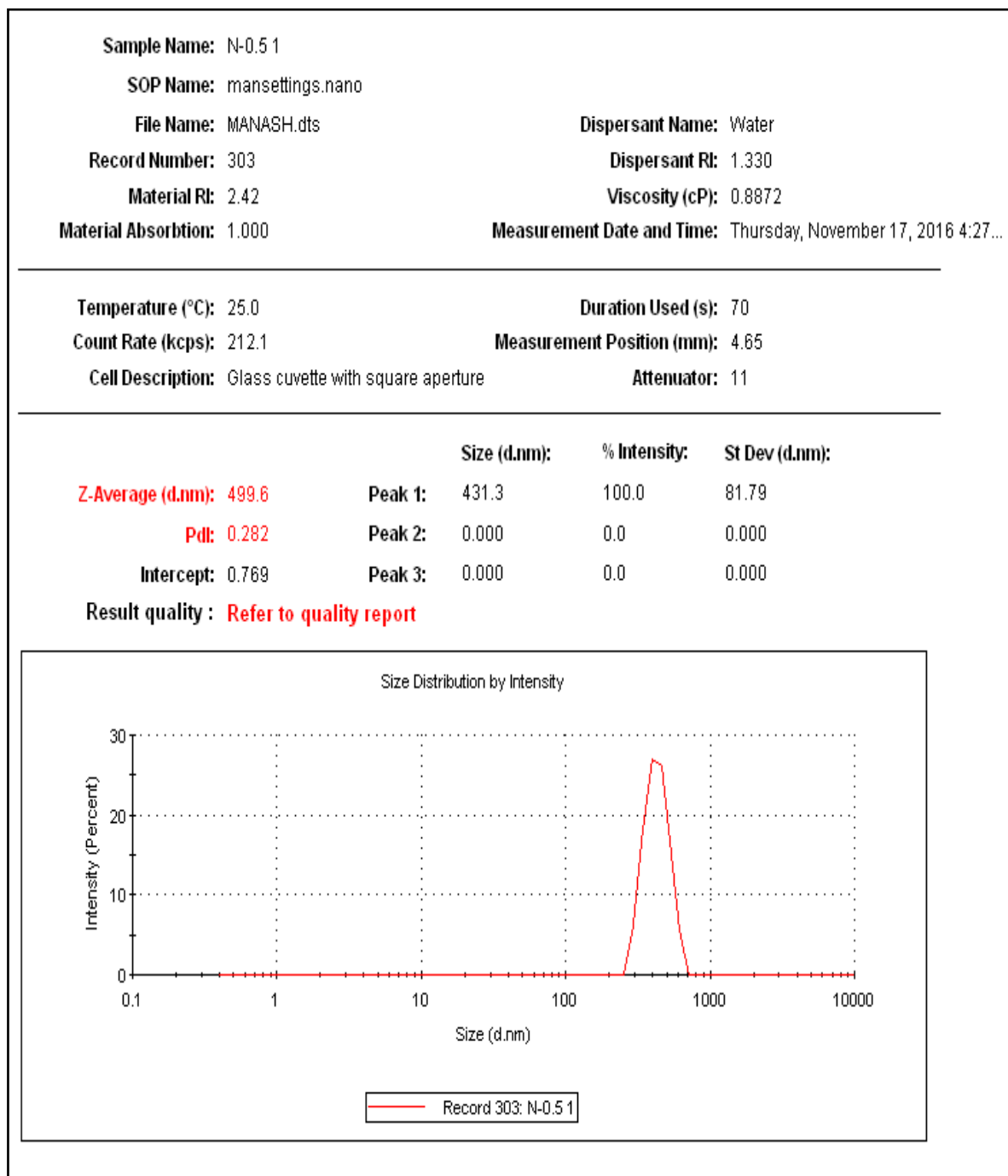


Fig.9b PDI value for the coated nanoparticles.

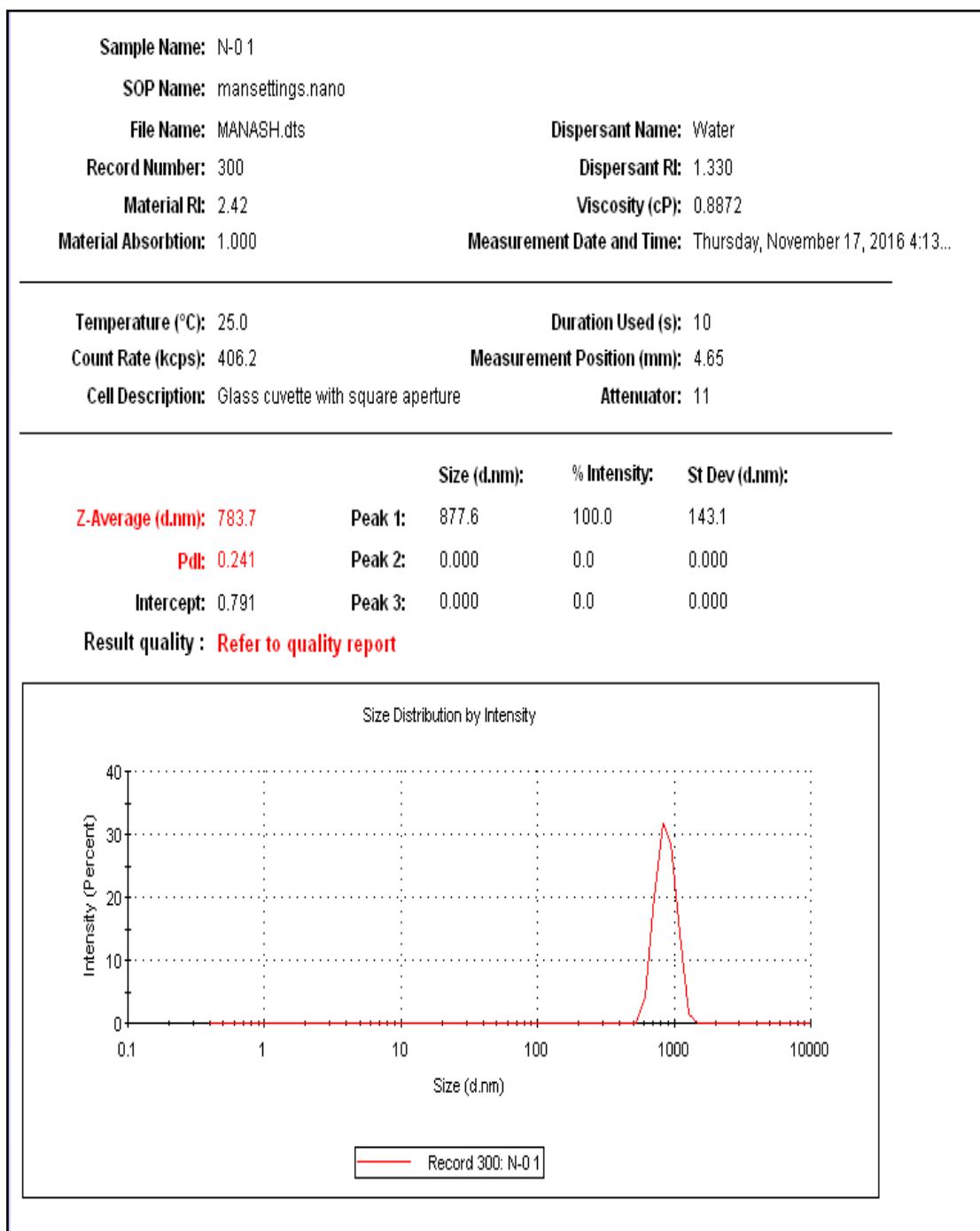


Fig.10 Drug release pattern of the curcumin loaded pectin coated iron oxide nanocomposite.

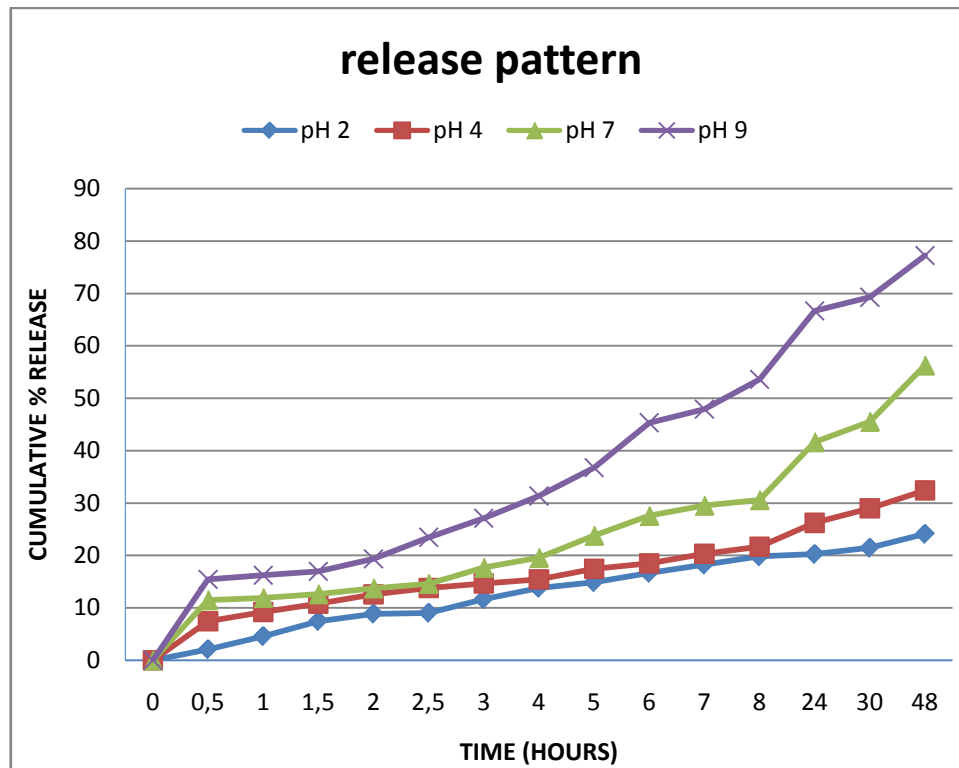


Table 1 Comparison between stability of colloids and the  $\zeta$  potential values.

potential [mV]	Colloid stability
$\pm[0, 5]$	Aggregation
$\pm[10, 30]$	High instability
$\pm[30, 40]$	Moderate stability
$\pm[40, 60]$	Good stability
$\geq 60$	Excellent stability

Table 2 Different formulations and their loading and encapsulation efficiency.

Sample	$\text{Fe}^{3+} / \text{Fe}^{2+}$	Pectin concentration (% w/v)	% yield	L%	EE%	
N-0	2:1	0.0	80			
N-0.3	2:1	0.3	36.74	15.4	13.5	
N-0.5	2:1	0.5	49.71	19.66	18.52	√
N-0.8	2:1	0.8	46.57	21.4	14.73	